Tight Sequestration of BH3 Proteins by BCL-xL at Subcellular Membranes Contributes to Apoptotic Resistance

Jessie Pécot, Laurent A Maillet, Janic P Le Pen, Céline Vuillier, Sophie de Carné Trécesson, Aurélie Fétiveau, Kristopher A Sarosiek, Florian J Bock, Frédérique Braun, Anthony A Letai, et al.

Cell Reports

Article

Tight Sequestration of BH3 Proteins by BCL-xL at Subcellular Membranes Contributes to Apoptotic Resistance

Jessie Pécot,[1,5] Laurent Maillet,[1,5] Janic Le Pen,[1] Céline Vuillier,[1] Sophie de Carné Trécesson,[1,6] Aurélie Fétiveau,[1] Kristopher A. Sarosiek,[3] Florian J. Bock,[4] Frédérique Braun,[1,7] Anthony Letai,[3] Stephen W.G. Tait,[4] Fabien Gautier,[1,2,*] and Philippe P. Juin[1,2,8,*]

[1]CRCNA, INSERM, CNRS, Université d'Angers, Université de Nantes, 44035 Nantes, France
[2]ICO René Gauducheau, 44805 Saint Herblain, France
[3]Dana-Farber Cancer Institute, Harvard Medical School, Boston, MA 02215, USA
[4]Cancer Research UK Beatson Institute, Institute of Cancer Sciences, University of Glasgow, Garscube Estate, Switchback Road, Glasgow G61 1BD, UK
[5]Co-first author
[6]Present address: Oncogene Biology Laboratory, The Francis Crick Institute, 1 Midland Road, NW1 1AT London, UK
[7]Present address: CNRS FRE3630 (affiliated with Université Paris-Diderot, Sorbonne Paris Cité), Institut de Biologie Physio-chimique, 13 rue Pierre et Marie Curie, 75005 Paris, France
[8]Lead Contact
*Correspondence: fabien.gautier@univ-nantes.fr (F.G.), philippe.juin@univ-nantes.fr (P.P.J.)
http://dx.doi.org/10.1016/j.celrep.2016.11.064

SUMMARY

Anti-apoptotic BCL-2 family members bind to BH3-only proteins and multidomain BAX/BAK to preserve mitochondrial integrity and maintain survival. Whereas inhibition of these interactions is the biological basis of BH3-mimetic anti-cancer therapy, the actual response of membrane-bound protein complexes to these compounds is currently ill-defined. Here, we find that treatment with BH3 mimetics targeting BCL-xL spares subsets of cells with the highest levels of this protein. In intact cells, sequestration of some pro-apoptotic activators (including PUMA and BIM) by full-length BCL-xL is much more resistant to derepression than previously described in cell-free systems. Alterations in the BCL-xL C-terminal anchor that impacts subcellular membrane-targeting and localization dynamics restore sensitivity. Thus, the membrane localization of BCL-xL enforces its control over cell survival and, importantly, limits the pro-apoptotic effects of BH3 mimetics by selectively influencing BCL-xL binding to key pro-apoptotic effectors.

INTRODUCTION

The BCL-2 family proteins are major regulators of mitochondrial outer membrane permeabilization (MOMP) and subsequent apoptosis in response to bacterial infection, immune responses, intrinsic tumor suppression, and anti-cancer therapy. This family functions as a network of interacting proteins where anti-apoptotic proteins oppose multidomain and BH3-only pro-apoptotic proteins. Anti-apoptotic proteins (including BCL-2, BCL-xL, and MCL-1) share four BCL-2 homology domains (BH1–BH4). They localize preferentially at intracellular membranes, predominantly the outer mitochondrial membrane, due to their hydrophobic C-terminal anchor (Juin et al., 2013). Multidomain pro-apoptotic proteins (BAX and BAK) only have three BH domains (BH1–BH3). They are produced mainly as inactive proteins that localize either in the cytosol or at the mitochondria and, upon activation, insert into mitochondrial membranes, where they trigger MOMP. BH3-only proteins (including BIM, BID, and PUMA) trigger apoptosis upstream of BAX/BAK. Some of them (such as BIM or PUMA) interact with mitochondria by themselves because they harbor specific targeting domains in their sequence (Wilfling et al., 2012). BH3-only proteins act as stress sensors and are activated transcriptionally, translationally, and/or post-translationally by numerous stimuli.

Induction of MOMP by pro-apoptotic BCL-2 members occurs through an ordered series of molecular events in which BH3 domains play a critical role. BAX/BAK, essential effectors of MOMP in mammalian cells, permeabilize mitochondrial membranes as active oligomers. Oligomerization is initiated by a nucleating dimer formed by the binding of the BH3 domain of one molecule into a hydrophobic groove formed by the BH1, -2, and -3 domains of a second molecule (Dewson et al., 2009, 2012). The BH3 domain is buried in inactive BAX/BAK, and its exposure is required for this dimerization (Czabotar et al., 2013; Moldoveanu et al., 2014). Such exposure is favored by the direct interaction of the BH3 domain of a subset of *activator* BH3-only proteins (namely, these of BID, BIM, or PUMA) with BAX (possibly at two sites; Gavathiotis et al., 2008; Czabotar et al., 2013) and BAK. Activation of BAX/BAK is thus initiated by a ligand-induced process that mitochondrial membranes also contribute to (Leber et al., 2010).
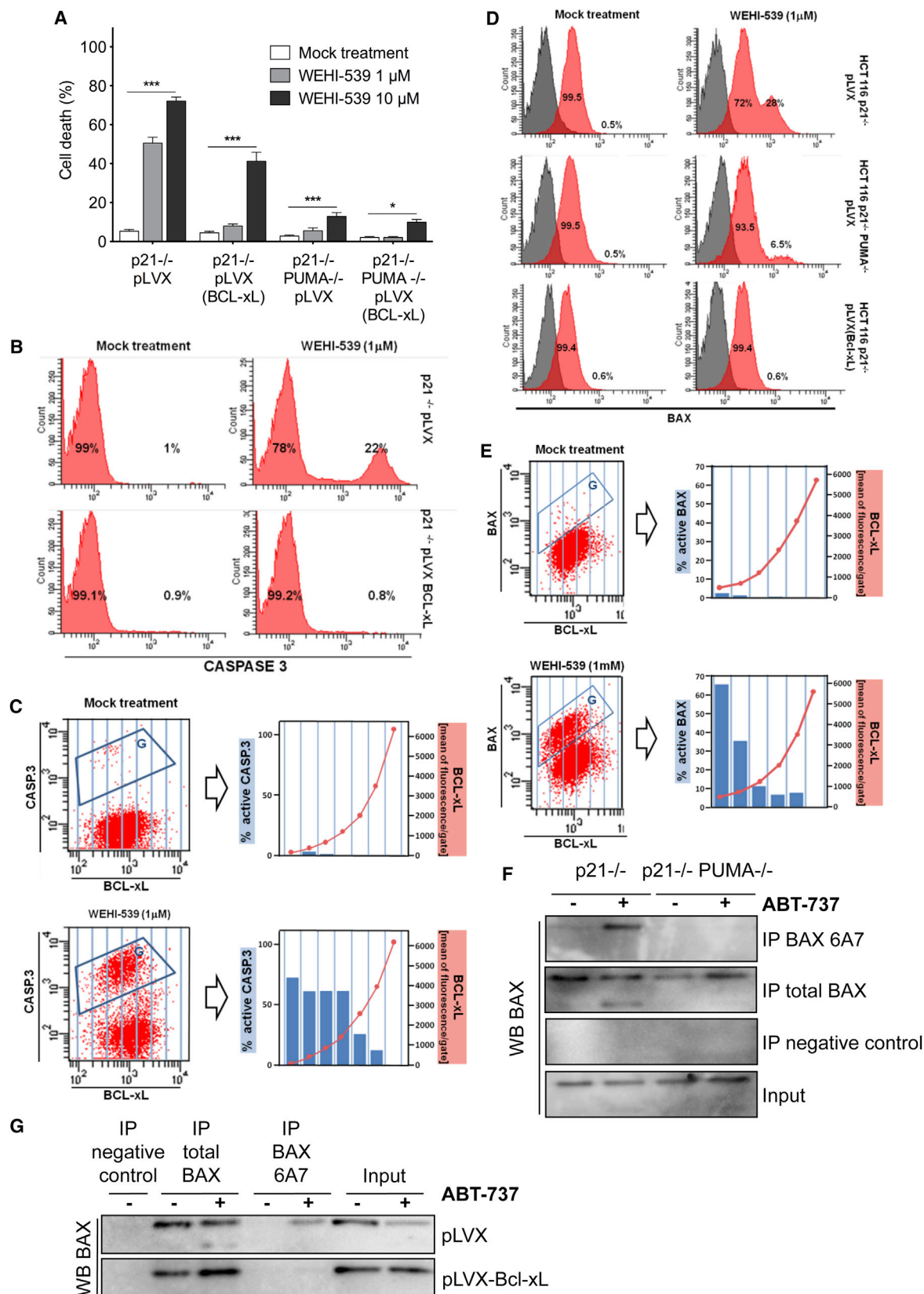
(legend on next page)

Anti-apoptotic BCL-2 proteins inhibit MOMP by competing with BAX/BAK to bind to activator BH3-only proteins and themselves (Billen et al., 2008; Chen et al., 2015). They do so in great part by engaging BH3 domains of the former and the latter at the level of a hydrophobic groove that is structurally similar to that mentioned above in BAX/BAK, but they form a more stable complex upon binding. This is negatively regulated by *sensitizer* BH3-only proteins that only interact with the BH3 binding sites of BCL-2 homologs, not with BAX/BAK. There are notable differences in the BH3 binding sites of BCL-2, BCL-xL, and MCL-1 that explain why they engage in preferential interactions with sensitizer BH3-only proteins and BAX/BAK. Therefore, they exert complementary differentially-regulated survival activities. These proteins are frequently overexpressed in cancer cells, so intrinsic tumor-suppressor pathways and conventional therapy fail to trigger BAX/BAK activation. Thus, compounds that would overcome these effects are of major interest. *BH3 mimetics* inhibitors (ABT-737 or ABT-263, which target BCL-2, BCL-xL, and BCL-w or WEHI-539, which selectively target BCL-xL) have been designed based on their ability to selectively occupy the BH3 binding sites of specific subsets of BCL-2 homologs, and some have entered clinical trials. These compounds are also powerful cell-permeant probes that help us understand how the BH3 binding activities of distinct BCL-2 homologs regulate survival in a whole-cell context.

Targeting BCL-xL is critical for cancer treatment because this protein is widely overexpressed in cancers, it binds to a wider range of pro-apoptotic proteins than any other known BCL-2 homologs, and its expression is a marker of chemoresistance (Amundson et al., 2000; Wei et al., 2012). The on-target dose-limiting effects of BH3 mimetics on platelet survival indicate that pharmacological inhibition of BCL-xL can be achieved by these compounds in vivo (Wilson et al., 2010). However, some studies hinted that BH3 mimetics might not fully inhibit intracellular BCL-xL in cancer cells (Mérino et al., 2012; Rooswinkel et al., 2012). The reason for this lack of efficiency, which implies that survival regulation by BCL-xL is tighter than expected, is currently unclear. In this study, using whole-cell systems, we show that the cell survival activity of BCL-xL is only partly antagonized by BH3 mimetics. Intracellular interactions between BCL-xL and a subset of pro-apoptotic proteins (including the activators PUMA and BIM) resist BH3 binding inhibition more than anticipated from preceding studies using soluble forms of BCL-xL generally assumed to be fully BH3-binding competent.

The robustness of PUMA/BCL-xL interactions, in particular, prevents BH3 mimetics from exploiting PUMA's ability to trigger BAX-dependent cell death, and this is likely to limit their effect in a chemotherapeutic setting because PUMA and BAX play a role in chemotherapy-induced apoptosis (Jeffers et al., 2003). We show that sequestration of pro-apoptotic proteins by BCL-xL is favored by its membrane binding and low-level mitochondrial translocation dynamics. This explains why membrane-localized BCL-xL has enhanced anti-apoptotic properties (including in response to BH3 mimetics) and establishes that intracellular localization of BCL-xL, per se, is critical for survival regulation.

RESULTS

BCL-xL-Mediated Inhibition of PUMA-Induced BAX-Mediated Cell Death Is Only Partly Derepressed by BH3 Mimetics

To investigate how efficiently the anti-apoptotic function of intracellular BCL-xL is antagonized by inhibition of its BH3 binding, we first evaluated how variations in BCL-xL expression impact cell-death induction by cell-permeant BH3 mimetics. We essentially employed HCT116 p21$^{-/-}$ cells; these cells die upon depletion of BCL-xL by RNA interference and thus represent a model of BCL-xL-dependent cells (Cartron et al., 2004; Gallenne et al., 2009). We used a HCT116 p21$^{-/-}$ cell line expressing endogenous BCL-xL ("control cells": HCT116 p21$^{-/-}$ pLVX) and a cell line stably expressing an average 4-fold increase in BCL-xL expression ("BCL-xL high expresser cells": HCT116 p21$^{-/-}$ pLVX(BCL-xL)) (Figure S1). BH3 profiling assays support earlier findings that these cells are dependent on BCL-xL survival function (Figure S1).

As shown in Figure 1A, treatment with WEHI-539 triggered cell death in a fraction of control HCT116 p21$^{-/-}$ cells. BCL-xL high-expresser cells resisted significantly more, even when concentrations of WEHI-539 as high as 10 μM were used (Figure 1A). Although the survival activity of BCL-xL can be derepressed by BH3 mimetics treatment of whole cells, derepression is therefore only partial and is counteracted by a relatively modest enhancement of BCL-xL expression.

We explored further whether cell-to-cell variations in BCL-xL expression might account for fractional killing by BH3 mimetic treatment. To investigate this, we performed intracellular immunostaining of HCT116 p21$^{-/-}$ pLVX cells to concomitantly

Figure 1. BCL-xL Levels Critically Determine Induction of PUMA-Dependent Cell Death by BH3 Mimetics

(A) The indicated HCT116 cell lines were treated with WEHI-539 (48 hr), and cell death was assessed using trypan blue exclusion assays.

(B) Flow cytometry analysis of the indicated HCT116 cell lines were treated with WEHI-539 (1 μM, 24 hr) and stained using anti-active Caspase-3-Alexa-647 antibodies.

(C) The relationship between BCL-xL expression and active Caspase-3 was determined by dividing dot plots resulting from intracellular immunostaining for BCL-xL and active Caspase-3 of HCT116 p21$^{-/-}$ pLVX cells (treated with WEHI-539 as in B) into vertical gates to grade BCL-xL expression (the red line indicates [mean of fluorescence per gate]). The percent of active Caspase-3 was defined for each vertical gate by enumerating the number of cells in the gate G intersected with each of the vertical gates. Data presented are representative of three independent experiments.

(D) Flow cytometry analysis of the indicated HCT116 cell lines treated with WEHI-539 (1 μM, 24 hr) and stained with anti-BAX-Alexa-647 antibodies.

(E) The relationship between BCL-xL expression and a subset of active BAX was determined by double intracellular staining, as described in Figure 1C.

(F) The indicated HCT116 cell lines were treated with ABT-737 (1 μM, 16 hr) prior to immunoprecipitation with a control, an anti-BAX, or an anti-BAX 6A7 antibody and western blot analysis.

(G) HCT116 p21$^{-/-}$ PUMA$^{-/-}$ pLVX and HCT116 p21$^{-/-}$ PUMA$^{-/-}$ pLVX(BCL-xL) were treated with ABT-737 (1 μM, 16 hr) before immunoprecipitation with a control, an anti-BAX, or an anti-BAX6A7 antibody and western blot analysis.

measure BCL-xL expression and cleavage of Caspase-3 (as a marker of apoptosis induction) on a single-cell basis after their treatment with WEHI-539. As shown in Figure 1B, no detectable cleaved Caspase-3 was measured in untreated HCT116 p21$^{-/-}$ pLVX cells, with an immunostaining that was equivalent to that obtained with a negative isotopic control (data not shown). Treatment with WEHI-539 of HCT116 p21$^{-/-}$ pLVX cells lead to the emergence of a subpopulation that stained positive for cleaved caspase 3, which was not observed when HCT116 p21$^{-/-}$ pLVX(BCL-xL) were treated (Figure 1B). Treatment of the sensitive HCT116 p21$^{-/-}$ pLVX cell population with WEHI-539 did not change the global log-normal distribution of BCL-xL expression levels (data not shown). Yet, thorough single-cell examination of the percentage of cleaved Caspase-3-positive cells as a function of the range of BCL-xL expression showed that activation of Caspase-3 occurred preferentially in cells expressing BCL-xL levels below the mean level (Figure 1C). Thus, cell-to-cell differences in the expression of BCL-xL levels, even in an apparently *homogenous* cell population, determine the response to a given BH3 mimetic treatment over a defined period of time.

To investigate the level at which the apoptotic cascade BCL-xL exerts a BH3 mimetic-resistant control, we investigated the effects of varying levels of BCL-xL on BAX activation. The latter pro-apoptotic multidomain effector indeed plays a major role in cell-death induction of our model HCT116 p21$^{-/-}$ cell line upon BCL-xL depletion and ABT-737 or WEHI-539 treatment (Gallenne et al., 2009; data not shown). When we performed BAX intracellular staining assays, we found that treatment of control HCT116 p21$^{-/-}$ pLVX cells lead to the generation of a new population of cells that was strongly stained with the anti-BAX antibody (Figure 1D). This was not inhibited by treatment with the caspase inhibitor QVD-Oph (data not shown). We assume that this qualitative change in BAX immunostaining illustrates a change in the nature of its interaction with subcellular membranes and, thus, in its activation status, as previously described for BAK (Griffiths et al., 1999). We found that overexpression of BCL-xL prevented a change of the BAX immunostaining profile upon treatment (Figure 1D). Moreover, we performed intracellular immunostaining to concomitantly measure BAX activation and BCL-xL expression on a single-cell basis in WEHI-539-treated control HCT116 p21$^{-/-}$ cells. Single-cell examination, in WEHI-539 treated HCT116 p21$^{-/-}$ pLVX populations, of the percentage of cells highly positive for BAX as a function of the range of BCL-xL expression showed that qualitative changes in BAX immunostaining occurred preferentially in cells of the population that expressed the lowest levels of BCL-xL (Figure 1E). The influence of BCL-xL on conformational changes in BAX upon BH3 mimetic treatment was further documented by monitoring changes in the amino-terminus domain of BAX (that accompany its activation; Hsu and Youle, 1997) by immunoprecipitation assays with the 6A7 antibody (Figure 1F). As shown in Figure 1G, BH3 mimetic treatment enhanced the amount of 6A7-positive BAX molecules in control, but not in BCL-xL high-expresser, cells (Figure 1G). Thus, inhibition of the BH3 binding of BCL-xL does not efficiently relieve its control over BAX activation.

To understand the exact mechanism BCL-xL counteracts to prevent BH3 mimetic-induced BAX activation in our model cell line, it should be recalled that we showed that endogenous PUMA, but neither BID nor BIM, plays a key role upstream of BAX during cell death induced by BCL-xL depletion in HCT116 p21$^{-/-}$ cells (Gallenne et al., 2009). PUMA can directly promote BAX activation (Cartron et al., 2004; Ren et al., 2010; Du et al., 2011; Edwards et al., 2013; Hockings et al., 2015). Using bioluminescence resonance energy transfer (BRET) assays (as described below) to monitor BAX oligomerization in whole cells, we found that PUMA favors, whereas BCL-xL prevents, such assembly in a whole-cell context (data not shown). Moreover, BH3 profiling of HCT116 p21$^{-/-}$ PUMA$^{-/-}$ pLVX and HCT116 p21$^{-/-}$ PUMA$^{-/-}$ pLVX(BCL-xL) cells compared to that of PUMA-proficient cells showed differential and additive effects of enhanced BCL-xL expression and PUMA depletion on the apoptotic priming of HCT-116 p21$^{-/-}$ cells, arguing that PUMA provides an *activating* death signal that BCL-xL has to counteract as a BH3-binding protein to maintain survival (Figure S1). Consistently, PUMA-deficient cells showed decreased cell death rates (Figure 1A) and less BAX activation (Figures 1D and 1F) upon treatment with BH3 mimetics. As a whole, these data indicate that BCL-xL counteracts PUMA-induced BAX-mediated cell death by a process that BH3 mimetics only partly derepress. This was further substantiated by experiments using a PUMA-inducible cell line or cells where PUMA expression was induced by a genotoxic treatment (Figure S1).

Interactions of BCL-xL with PUMA or BAX in Intact Cells Show Differing Sensitivity to BH3 Binding Inhibition

The resistance of cells expressing the highest levels of BCL-xL to BH3 mimetic induction of cell death may simply reflect the fact that these compounds act as competitive inhibitors. Alternatively, it may result from the fact that BCL-xL exerts BH3 mimetic-resistant functions to prevent cell death and, in particular, antagonize PUMA-induced BAX activity. To explore this, we investigated whether some molecular interactions engaged by intracellular BCL-xL would be particularly resistant to derepression using a bioluminescence resonance energy transfer (BRET) approach (Le Pen et al., 2016). BRET assays allowed us to evaluate, within whole live cells, the close proximity between two proteins by measuring energy transfer (upon addition of a luciferase substrate) between RLuciferase (RLuc; as a donor, fused to one protein) and yellow fluorescent protein (YFP; as an acceptor, fused to the other). To confirm that BRET signals testify specific interactions and do not result from random collisions, we systematically evaluated, following previously published rules (Pfleger and Eidne, 2006), the saturable nature of signals observed between a given level of donor and increasing levels of acceptor. To establish the necessity for BCL-xL to have a fully intact BH3 binding site to engage in live-cell interactions, we used a BCL-xL variant (BCL-xL G138E R139L I140N) carrying three mutations in the BH1 domain, which is critical for BH3 binding (Kim et al., 2006).

We first focused on interactions engaged with PUMA. As shown in Figure 2A, saturable and strong BRET signals were observed in HCT116 p21$^{-/-}$ pLVX cells between RLuc fused to the N-terminal end of PUMA and YFP fused to the N-terminal end of BCL-xL. Interactions between corresponding proteins were confirmed in co-immunoprecipitation assays (Figure 2B).
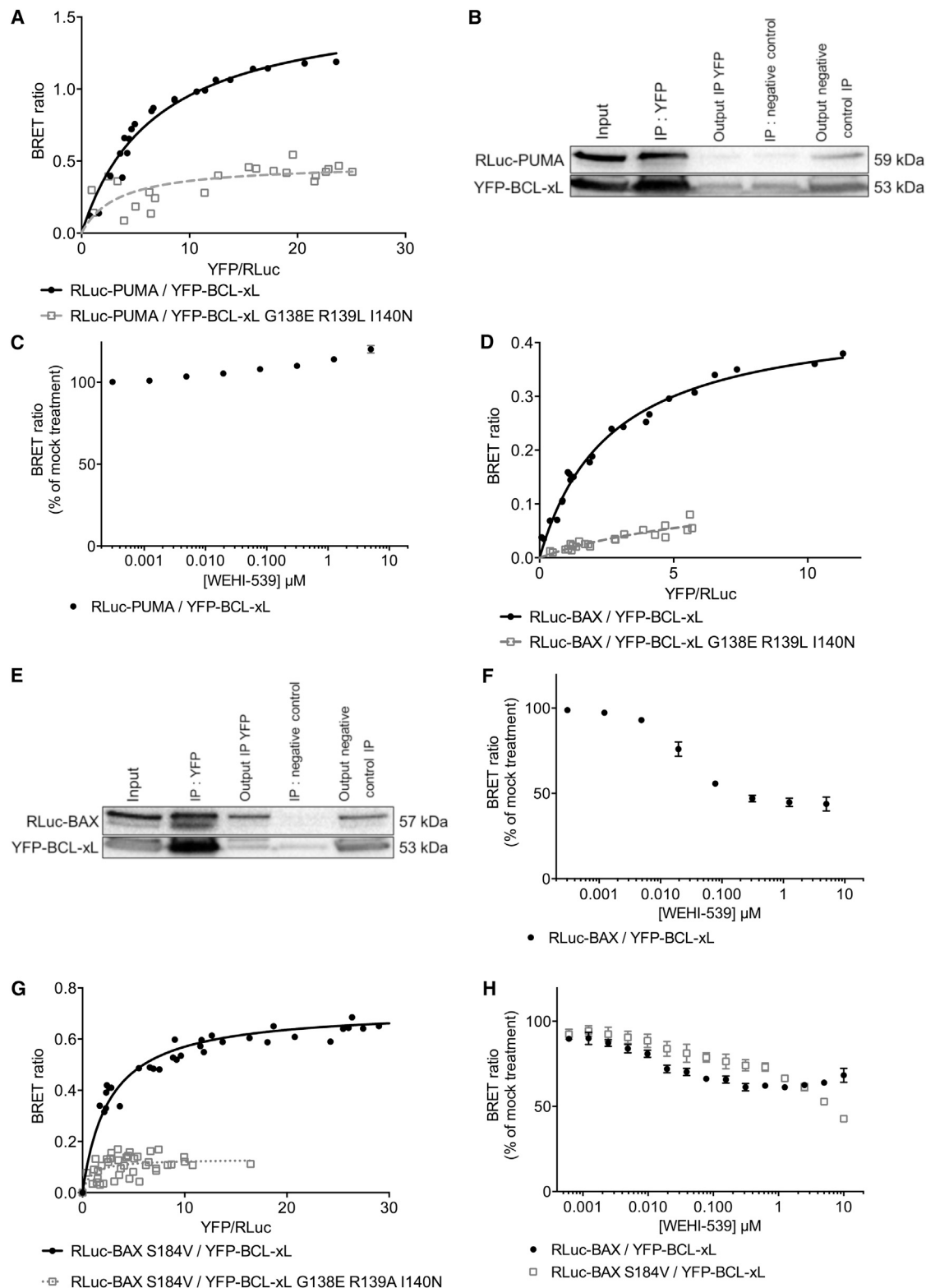
Figure 2. BH3 Mimetics Do Not Inhibit Interactions of Full-Length BCL-xL with PUMA

(A) BRET saturation assay analysis was performed in HCT116 p21$^{-/-}$ pLVX cells using an increasing amount of vectors encoding for YFP-BCL-xL, or YFP-BCL-xL G138E, R139L, I140N in the presence of a fixed amount of the vector-encoding RLuc-PUMA. BRET ratios were measured for every YFP-BCL-xL plasmid

(legend continued on next page)

BRET signals were much weaker between PUMA and BCL-xL G138E R139L I140N (Figure 2A). Strikingly, we observed no inhibitory effect of up to 10 μM of WEHI-539 on PUMA/BCL-xL interactions in whole cells (Figure 2C). Likewise, ABT-737 treatment had no detectable effect (data not shown). Similar observations were made using MCF-7 cells (Figures S2A and 3B). To further confirm the resistance of PUMA/BCL-xL interactions in a cellular context that lacks any other member of the BCL-2 family, we used yeast ectopically expressing these proteins fused to RLuc and YFP. PUMA/BCL-xL BRET signals measured in yeast were also refractory to BH3 mimetic treatment (Figure S2B).

We reasoned that, since BH3 mimetic can trigger PUMA-mediated BAX-dependent cell death in some instances, some vulnerable complexes had to exist in the PUMA/BAX/BCL-xL network. We thus measured the effects of BH3 mimetics on BAX/BCL-xL interactions. As shown in Figure 2D, and consistent with preceding results (Bah et al., 2014), saturable BRET signals were observed in HCT116 p21$^{-/-}$ pLVX cells between RLuc fused to the N-terminal end of BAX and increasing levels of YFP-BCL-xL. Interactions were confirmed in co-immunoprecipitation assays (Figure 2E). Saturable BRET signals were not observed between RLuc-BAX and YFP-fused BCL-xL G138E R139L I140N (Figure 2D). In contrast to what we observed with PUMA, BRET signals were inhibited by WEHI-539 in a dose-dependent manner, with concentrations as low as 10 nM having an effect, and an apparent median effective concentration in the 25 nM order (Figure 2F). Experiments using ABT-737 and equivalent amounts of YFP-BCL-xL gave qualitatively comparable results. They were consistent with the notion that this compound is less efficient at targeting BCL-xL than WEHI-539 (Figure S2C) (Lessene et al., 2013). ABT-199 had no detectable effect on BAX/BCL-xL BRET signals (data not shown). Similar results were obtained using MCF-7 cells instead of HCT116 cells (see below). BAX/BCL-xL interactions in yeast cells were also sensitive to BH3 mimetic treatment (Figure S2B).

Fusion of YFP, whose size is comparable to that of RLuc, to the N-terminal end of BAX generates a protein that partitions between the cytosol and the mitochondria (data not shown). Thus, we assume that this is also the case for RLuc-BAX. To investigate whether membrane insertion of BAX (a key step during the course of its activation) affects the nature of its interactions with BCL-xL, we used BAX S184V, a mutant that is constitutively bound to and inserted into mitochondrial membranes (Nechushtan et al., 1999; Schellenberg et al., 2013). Saturable BRET signals were still observed between BAX S184V and

BCL-xL (Figure 2G). However, the corresponding BRET signals remained sensitive to derepression, even if higher concentrations of compounds were required to inhibit them (Figure 2H). These data indicate that membrane-inserted BAX interacts with full-length BCL-xL, but that sequestration can be derepressed.

Membrane-Bound BCL-xL Resists Inhibition

When studied in solution, the interaction between PUMA and BCL-xL appears to be sensitive to BH3 mimetics (Gautier et al., 2011 and references therein). Thus, we reasoned that the resistance of cellular interactions revealed in the above assays might ensue from the localization of full-length BCL-xL at intracellular membranes. To test this hypothesis, we reiterated BRET assays using YFP-fused BCL-xL deleted in its C-terminal end. The resulting protein, in contrast to full-length BCL-xL, had a cytosolic localization (BCL-xL ΔC) (Figure S3A) Saturable BRET signals were observed only between RLuc-PUMA and YFP-BCL-xL ΔC, and not between RLuc-PUMA and YFP-fused BCL-xL G138E R139L I140N ΔC (Figure 3A). Most strikingly, when we evaluated the effect of a range of WEHI-539 concentrations on PUMA/BCL-xL-ΔC BRET signals, we found that these interactions were significantly sensitive to WEHI-539 treatment, with concentrations as low as 10 nM having an effect, and an apparent median effective concentration in the 100 nM order (Figure 3B). Notably, as shown in Figures 3B and S3A, WEHI-539 also affected interactions between PUMA and a cytosolic variant of BCL-xL only carrying a point mutation (A221R) in the C-terminal end (Garenne et al., 2016). This argues that the enhanced sensitivity of BCL-xL-ΔC interactions results from a lack of membrane integration, not from a membrane-independent role the C-terminal end would play in the regulation of BH3 binding. HCT116 p21$^{-/-}$ cells overexpressing cytosolic BCL-xL ΔC and A221R did not resist treatment with 1 μM of WEHI-539, establishing that membrane localization of BCL-xL significantly contributes to its resistance to derepression (Figures 3C and S3B).

Steady-state levels of BCL-xL at subcellular membranes result from a dynamic equilibrium between membrane targeting and retro-translocation rates. Retro-translocation is an ill-characterized process whereby membrane-bound BCL-xL is shuttled back to the cytosol (Edlich et al., 2011). BRET signals between RLuc-PUMA and YFP fused to a variant of BCL-xL (BCL-xL Δ2) that exhibited partial mitochondrial localization and increased retrotranslocation rates (Figure S3A; Todt et al., 2013) were nearly as sensitive to WEHI-539 treatment than those observed using cytosolic variants of BCL-xL (Figure 3B).

concentration and are plotted as a function of the ratio of total acceptor fluorescence to donor luminescence. The data were fitted using a nonlinear regression equation assuming a single binding site.

(B) HCT116 p21$^{-/-}$ pLVX were transfected with vectors encoding RLuc-PUMA and YFP-BCL-xL before lysis, and immunoprecipitation with a negative control or an anti-GFP antibody followed by western blot analysis with RLuc and YFP antibodies.

(C) WEHI-539 response of RLuc-PUMA/YFP-BCL-xL BRET signals was assessed by concentration curve experiments in the HCT116 p21$^{-/-}$ pLVX cell line. Data are presented as mean ± SEM of three independent experiments.

(D) BRET saturation assay analysis was performed as described in Figure 2A, using YFP-BCL-xL and RLuc-BAX.

(E) Immunoprecipitation assays were performed as in Figure 2B.

(F) The response of RLuc-BAX/YFP-BCL-xL to WEHI-539 treatment was assessed as described in Figure 2C.

(G) BRET saturation assay analysis was performed in MCF-7 cells as described in Figure 2A, using RLuc-BAX S184V as a donor.

(H) The WEHI-539 response of RLuc-BAX/YFP-BCL-xL and Rluc-BAX S184V/YFP-BCL-xL was assessed by concentration curve experiments in the MCF-7 cell line.
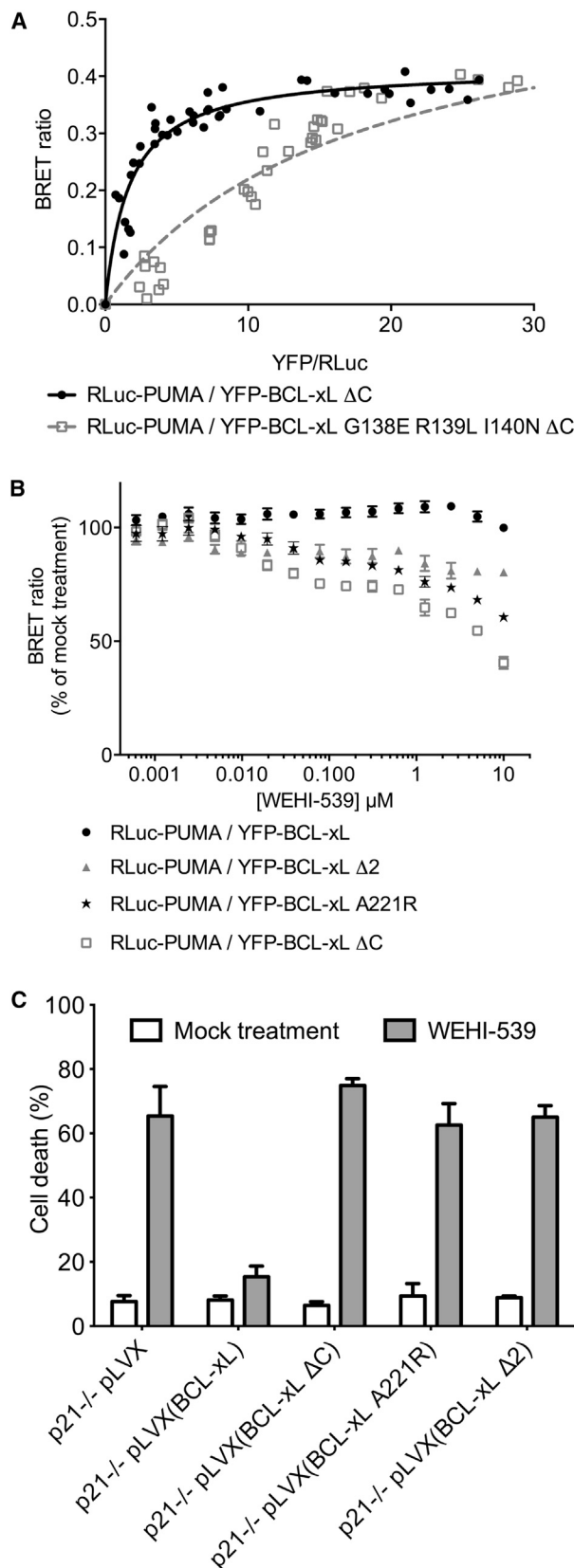
Figure 3. Membrane-Bound BCL-xL Resists Derepression

(A) BRET saturation curve assays using RLuc-PUMA/YFP-BCL-xLΔC or YFP-BCL-xLG138E, R139L, I140N were performed in MCF-7 cells. The data were fitted using a nonlinear regression equation assuming a single binding site. Data presented are representative of three independent experiments.

(B) Sensitivity of interactions between RLuc-PUMA and YFP-BCL-xL or YFP fused to BCL-xL variants (A221R, Δ2, and ΔC) to WEHI treatments were assessed using concentration curve experiments in MCF-7 cells. Data are presented as mean ± SEM of three independent experiments.

(C) Cell-death assays were performed as indicated in Figure 1A, using the indicated HCT116 p21$^{-/-}$ cell lines treated with WEHI-539 or ABT-199 (1 μM, 16 hr).

Moreover, HCT116 p21$^{-/-}$ cells overexpressing cytosolic BCL-xL Δ2 did not resist treatment with 1 μM of WEHI-539. Thus, membrane localization dynamics influence the tightness of BCL-xL BH3 binding.

Of note, the fact that PUMA/BCL-xL interactions may only be sensitive to derepression when interactions with membranes are weakened implies that cell solubilization used in classical co-immunoprecipitation assays can artificially impair these interactions, leading to an overestimation of the effects of derepression. In agreement with this, and consistent with preceding data (Gautier et al., 2011), an effect of BH3 mimetic treatment on PUMA/BCL-xL interactions was detected upon co-immunoprecipitation from HCT116 p21$^{-/-}$ cell lysates, but not when more abundant complexes were investigated using HCT116 p21$^{-/-}$ pLVX(BCL-xL) cell lysates (Figure S3C).

We eventually investigated whether membrane localization impacts the intracellular interactions of BCL-xL with other pro-apoptotic proteins of the BCL-2 family (namely BAX, BAK, BIM$_L$, BAD, and tBID). We compared sensitivities of corresponding validated BRET signals obtained with full-length or C-terminal-deleted BCL-xL to BH3 mimetics (Figures 4A and S4). We made two findings. First, we observed that BIM$_L$/BCL-xL interactions are, akin to PUMA/BCl-xL, almost completely resistant to derepression by BH3 mimetics. In contrast, interactions with BAD, BAK, and tBID showed differing sensitivities, with the latter interaction being the most sensitive one. To confirm that the prevalence of sensitive protein complexes impacts sensitivity to death induced by BCL-xL inhibition, we used recently described *mito-primed* cells engineered to coexpress ectopic BCL-xL and either tBID or PUMA (Lopez et al., 2016), and we challenged them with WEHI-539. As shown in Figure 4B, BCL-xL-addicted tBID-expressing cells were significantly more sensitive than PUMA-expressing ones, despite enhanced expression of the latter pro-apoptotic protein compared to the former (see Lopez et al., 2016). Second, we observed that constraining BCL-xL cytosolic localization favored derepression of interactions with BAK, BAD, and BIM$_L$. This argues that membrane localization of BCL-xL has a general impact on its BH3 binding properties. Two notable exceptions were interactions with tBID and BAX, which were almost equally sensitive to BH3 mimetic treatment regardless of BCL-xL localization. The inherent cytosolic localization of BAX may play a role in the latter case, because interactions of membrane-inserted BAX S184V with BCL-xLΔC were more sensitive to derepression than those with full-length BCL-xL (Figure 4A).
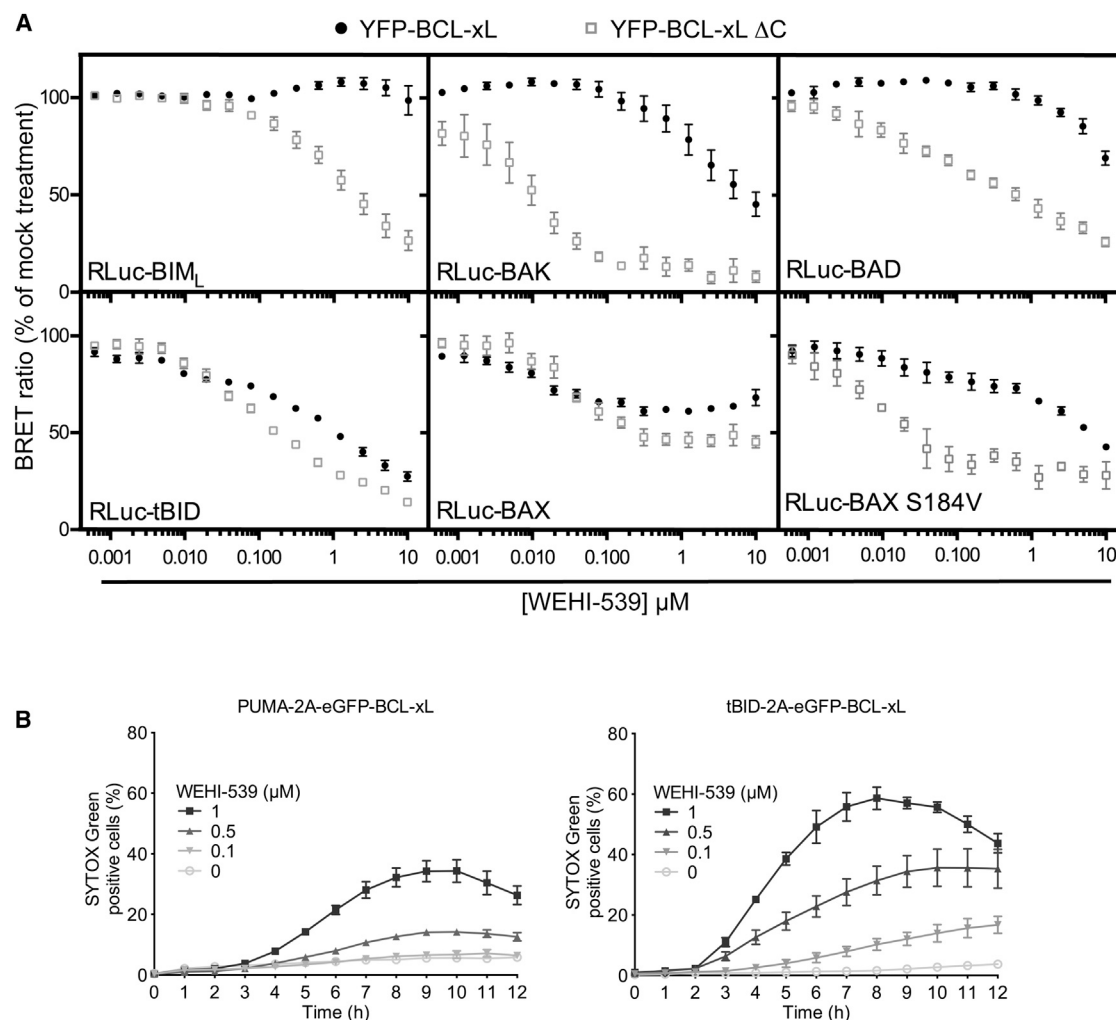
Figure 4. Sensitivity to Derepression of BCL-xL Complexes Depends on Membrane Localization and the Identity of the Pro-apoptotic Binding Partner

(A) WEHI-539 sensitivities of interactions between YFP-BCL-xL or YFP-xLΔC and RLuc fused to BIM$_L$, BAK, BAD, tBID, BAX, and BAX S184V were assessed by concentration curve experiments in the MCF-7 cell line as described in Figure 2C.
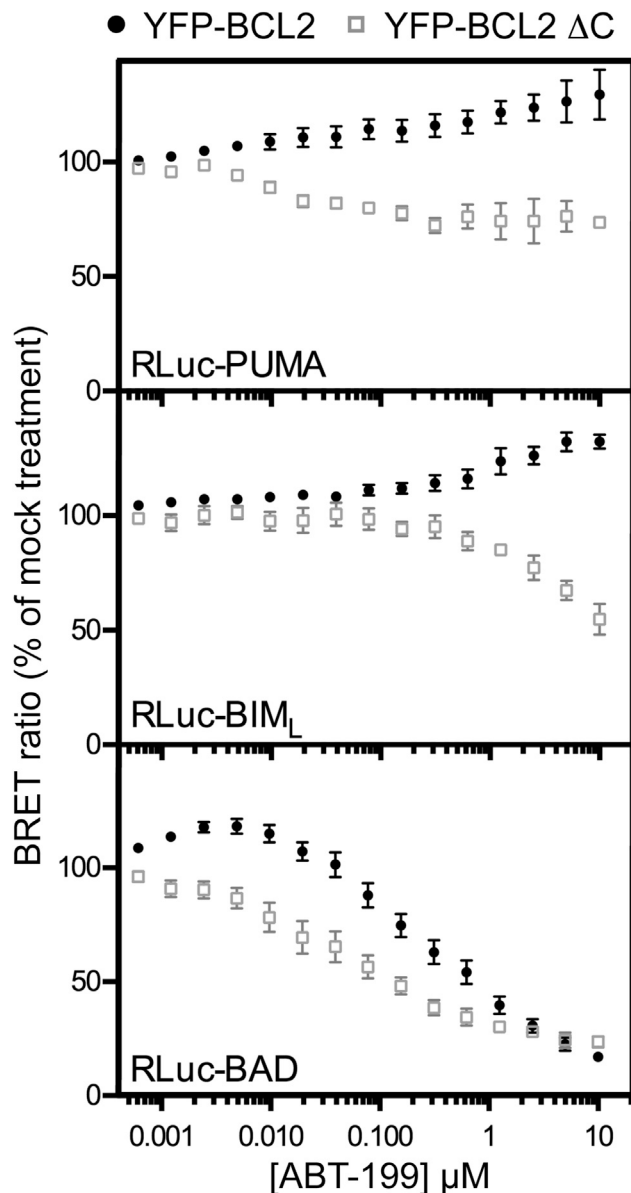
(B) The indicated BCL-xL-dependent cell lines were treated with the indicated concentration of WEHI-539 and analyzed over time for cell viability by SYTOX green dye exclusion and live-cell imaging using an IncuCyte imager. Data are mean ± SEM of three independent experiments.

DISCUSSION

In order to understand what determines MOMP onset, we need to understand how BCL-2 homologs respond to perturbations of their BH3 binding activity downstream of multiple stress signals. Our study points out that some anti-apoptotic effects of BCL-xL resist direct perturbations by BH3 mimetics. BH3 binding-site-independent survival properties of BCL-xL have been described and might contribute to this resistance (Follis et al., 2013 and references therein). BCL-xL may also impact the apoptotic balance by influencing the expression levels of its pro-apoptotic binding partners (Bertin-Ciftci et al., 2013). Consistent with this notion, we found a slight but significant decrease in BAX expression upon BCL-xL overexpression. This is, however, reverted by BH3 mimetic treatment, and it

is therefore unlikely to fully account for resistance (data not shown). Herein, we establish one more level of resistance by showing, using whole-cell assays that take into account membrane contribution, that intracellular interactions between BCL-xL and a subset of pro-apoptotic counterparts are more robust than preceding assays using soluble forms of BCL-xL lead us to expect.

Since PUMA and BIM$_L$ can function as pro-apoptotic activators upstream of multi-domain proteins, their maintained sequestration by full-length BCL-xL during BH3 mimetics treatment is expected to contribute to resistance. Our observations have therapeutic implications due to the role played by PUMA in the apoptotic response to genotoxic treatments and the contribution of BCL-xL to chemoresistance. They indicate that the anti-apoptotic activity exerted by overexpressed BCL-xL in

● YFP-BCL2   □ YFP-BCL2 ΔC

Figure 5. Deletion of the BCL-2 C-terminal End Sensitizes PUMA, BIML, and BAD Interactions to ABT-199 Treatment

Sensitivities of various BCL-2 interactions to ABT-199 were assessed by concentration curve experiments in the MCF-7 cell line between YFP-BCL-2 or BCL-2ΔC and RLuc fused to PUMA, BIM_L or BAD as described in Figure 2C.

fact that intracellular BCL-xL sequesters PUMA in a BH3 mimetic-resistant manner.

The binding of BCL-xL to subcellular membranes appears critical for its sequestration of PUMA and BIM_L, because corresponding interactions are profoundly affected by alterations in the C-terminal end of BCL-xL, which render this protein cytosolic, and concomitantly relieve resistance to cell-death induction by BH3 mimetics. It is sufficient to increase the retrotranslocation rates of BCL-xL to decrease its anti-apoptotic BH3 binding, underscoring that the BCL-xL network has to be considered as a dynamically evolving one in which synthesis and shuttling kinetics need to be taken into account. Our observations evoke the suggested enhanced sensitivity of cytosolic (compared to mitochondrial) pools of BIM_L/BCL-xL complexes to BH3 mimetics (Aranovich et al., 2012; Liu et al., 2012). Preceding studies proposed that membrane-bound BCL-xL would display a loosened groove structure in a hydrophobic environment and a lower affinity for BH3 domains (Bhat et al., 2012). Our data are more in agreement with a recent study that established that membrane-anchored BCL-xL binds better to BH3 domains than its isolated water-soluble moiety (Yao et al., 2015), possibly because the membrane environment of BCL-xL limits the dissociation rate (k_{off}) of its interactions. Cooperative interactions of BCL-xL and apoptotic ligands with the lipid bilayer membrane and cellular events that regulate BCL-xL integration in membranes may thus contribute to enforcement of BH3 binding (and BH3 mimetic resistance). Membrane localization of full-length BCL-xL in a whole-cell context may also permit post-translational modifications that contribute to this enhancement and that cell-free assays and recombinant proteins overlook. Importantly, membranes also appear to tighten the control BCL-2 exerts over cell death, because whole cell interactions with PUMA, BIM_L, and BAD were sensitized to ABT-199 by deletion of the BCL-2 C-terminal end (Figures 5 and S5).

The BCL-xL network of interactions has vulnerabilities because BH3 mimetics selectively targeting BCL-xL trigger cell death in some instances. Interactions of intracellular full-length BCL-xL with tBID (consistent with Aranovich et al., 2012), or BAX (this study) are indeed particularly sensitive to derepression. These interactions are not further sensitized to BH3 mimetic treatment when BCL-xL is cytosolic. This suggests that their weakness might be due to a lack of membrane contribution to complex formation. Somehow consistent with this, BCL-xL interactions with membrane-embedded BAX S184V showed a resistance to derepression that was relieved by deletion of the BCL-xL C-terminal end. However, intracellular BAX S184V/BCL-xL interactions remained more sensitive than most other interactions. Thus, the control BCL-xL exerts over retrotranslocation-competent BAX (Edlich et al., 2011) and membrane-embedded BAX (Subburaj et al., 2015) can be derepressed.

Our data are mostly consistent with the dual engagement model proposed by Llambi et al. (2011), wherein anti-apoptotic proteins interact with distinct pro-apoptotic proteins by modes that differ in their anti-apoptotic efficiency and sensitivity to derepression. Inhibition of BH3 binding leads to cell death only when the balance between pro-apoptotic members and BCL-xL favors *fragile* complexes instead of *refractory* ones. These

chemotherapy-challenged cancer cells is not as pharmacologically tractable as anticipated from the cell-free performances of currently available BH3 mimetics. In fact, these efficiently target BCL-xL only in some contexts (including in platelets, owing to their dose-limiting thrombopenic effects; Mason et al., 2007; Lessene et al., 2013) and not in others, especially when BCL-xL expression is high in cells in receipt of a genotoxic treatment (van Delft et al., 2006; Rooswinkel et al., 2012; Mérino et al., 2012; Vogler et al., 2009; Colak et al., 2014; this study). We propose that this inefficiency ensues, at least in part, from the

authors suggested that interactions with multidomain proteins (MODE 2) are less easily derepressed than interactions with BH3 activators (MODE 1) using tBID as a BH3 activator. Because interactions with PUMA or BIM$_L$ are significantly more robust than those with tBID and with BAX or BAK, the sensitivity of MODE 1 may, in fact, strongly depend on the main activator BH3-only protein involved. In the specific case of PUMA-driven BAX activation, interactions engaged by BCL-xL are not equally well inhibited, and PUMA is less efficiently released from BCL-xL than BAX. As a result, enhanced BCL-xL, most likely by competing with BAX for binding to PUMA in a BH3 mimetic resistant manner, prevents these compounds from fully exploiting PUMA's ability to induce BAX oligomerization and activation. This appears to be so critical that cell-to-cell variations in BCL-xL expression levels critically determine the fate of cells upon derepression.

Understanding the molecular basis of fractional resistance to derepression and how sustainable this is may be all the more relevant because non-lethal perturbation of the BCL-2 network may lead to genomic instability (Ichim et al., 2015). Our work shows that experimental systems that take into account membrane contribution in a whole-cell configuration are required to fully appreciate how stimulation of the dynamic BCL-2 network of functionally distinct interacting partners leads to cell death. The BRET approach we describe is particularly apposite to do so and to define a model that incorporates the differences in binding affinities into the consequences for the cell response.

EXPERIMENTAL PROCEDURES

Reagents and cell culture materials, including mito-primed immortalized murine endothelial cells (SVECs) coexpressing BCL-xL and either tBID or PUMA using a 2A self-cleaving peptide sequence and BH3 profiling assays are described in the Supplemental Information.

Flow Cytometry Intracellular Staining
Cells were fixed in 1% paraformaldehyde (in PBS) for 10 min at room temperature (RT) and permeabilized in cold methanol for 30 min at 4°C. Next, cells were incubated with antibodies for 1 hr at 4°C in the dark; rabbit immunoglobulin G (IgG) isotype control Alexa 488 (#4340S), BCL-xL-Alexa 488 (#2767S), mouse IgG isotype control Alexa 647 (sc-24636), IgG Bax-647 (sc-20067), rabbit IgG isotype control Alexa-647 (USBio I1903-93), Caspase-3 Alexa-647 (Cell Signaling 9602), mouse IgG isotype control Alexa 488 (BioLegend 400129), IgG Bax Alexa 488 (NBP233092), mouse IgG isotype control Alexa 647 (NBP2-24979), and IgG mouse Bax6A7 Alexa 647 (NBP1-28566) were used. Cells were washed twice in PBS containing 0.5% BSA. Flow cytometry analysis was performed just after staining.

BRET Assays
RLuc expression plasmids were constructed by subcloning coding sequences into the pRLuc-C2 vector (BioSignal Packard). Enhanced YFP (eYFP) expression plasmids were constructed by subcloning coding sequences into the pEYFP-C1 vector (BD Biosciences). All constructs were sequenced before use. BRET saturation curve assays and concentration/response curve assays are described in the Supplemental Information.

Immunoprecipitation Assays
Cells treated in 10-cm petri dishes were collected and washed with PBS. Cell lysis was performed using PBS-1% CHAPS buffer (plus a cocktail of protease and phosphatase inhibitors), and cellular suspensions were sonicated for 15 min thrice. Immunoprecipitations were performed as described in the

PureProteome Protein G Magnetic Beads protocol (Millipore). Briefly, 10 μL of anti-BCL-xL, 5 μL of anti-BAX antibody (Dako), 10 μL of anti-BAX 6A7 antibody (Abcam), 2 μL of anti-GFP antibody (Abcam), or 5 μL of anti-Flag (Sigma) antibody were used for 500 μg of cell extract.

Data Analysis
Data were from at least three independent experiments. Statistical analysis of data was performed using one-way ANOVA, two-way ANOVA, or Mann-Whitney tests on GraphPad Prism. Error bars represent SEM. The following symbols *, ** and *** correspond to a p value inferior to 0.05, 0.01, and 0.001, respectively.

SUPPLEMENTAL INFORMATION

Supplemental Information includes Supplemental Experimental Procedures and five figures and can be found with this article online at http://dx.doi.org/10.1016/j.celrep.2016.11.064.

REFERENCES

Amundson, S.A., Myers, T.G., Scudiero, D., Kitada, S., Reed, J.C., and Fornace, A.J., Jr. (2000). An informatics approach identifying markers of chemosensitivity in human cancer cell lines. Cancer Res. 60, 6101–6110.

Aranovich, A., Liu, Q., Collins, T., Geng, F., Dixit, S., Leber, B., and Andrews, D.W. (2012). Differences in the mechanisms of proapoptotic BH3 proteins binding to Bcl-XL and Bcl-2 quantified in live MCF-7 cells. Mol. Cell 45, 754–763.

Bah, N., Maillet, L., Ryan, J., Dubreil, S., Gautier, F., Letai, A., Juin, P., and Barillé-Nion, S. (2014). Bcl-xL controls a switch between cell death modes during mitotic arrest. Cell Death Dis. 5, e1291.

Bertin-Ciftci, J., Barré, B., Le Pen, J., Maillet, L., Couriaud, C., Juin, P., and Braun, F. (2013). pRb/E2F-1-mediated caspase-dependent induction of Noxa amplifies the apoptotic effects of the Bcl-2/Bcl-xL inhibitor ABT-737. Cell Death Differ. 20, 755–764.

Bhat, V., McDonald, C.B., Mikles, D.C., Deegan, B.J., Seldeen, K.L., Bates, M.L., and Farooq, A. (2012). Ligand binding and membrane insertion compete with oligomerization of the BclXL apoptotic repressor. J. Mol. Biol. 416, 57–77.

Billen, L.P., Kokoski, C.L., Lovell, J.F., Leber, B., and Andrews, D.W. (2008). Bcl-XL inhibits membrane permeabilization by competing with Bax. PLoS Biol. 6, e147.

Cartron, P.-F., Gallenne, T., Bougras, G., Gautier, F., Manero, F., Vusio, P., Meflah, K., Vallette, F.M., and Juin, P. (2004). The first alpha helix of Bax plays a necessary role in its ligand-induced activation by the BH3-only proteins Bid and PUMA. Mol. Cell 16, 807–818.

Chen, H.C., Kanai, M., Inoue-Yamauchi, A., Tu, H.C., Huang, Y., Ren, D., Kim, H., Takeda, S., Reyna, D.E., Chan, P.M., et al. (2015). An interconnected hierarchical model of cell death regulation by the BCL-2 family. Nat. Cell Biol. 17, 1270–1281.

Colak, S., Zimberlin, C.D., Fessler, E., Hogdal, L., Prasetyanti, P.R., Grandela, C.M., Letai, A., and Medema, J.P. (2014). Decreased mitochondrial priming determines chemoresistance of colon cancer stem cells. Cell Death Differ. 21, 1170–1177.

Czabotar, P.E., Westphal, D., Dewson, G., Ma, S., Hockings, C., Fairlie, W.D., Lee, E.F., Yao, S., Robin, A.Y., Smith, B.J., et al. (2013). Bax crystal structures reveal how BH3 domains activate Bax and nucleate its oligomerization to induce apoptosis. Cell 152, 519–531.

Dewson, G., Kratina, T., Czabotar, P., Day, C.L., Adams, J.M., and Kluck, R.M. (2009). Bak activation for apoptosis involves oligomerization of dimers via their alpha6 helices. Mol. Cell 36, 696–703.

Dewson, G., Ma, S., Frederick, P., Hockings, C., Tan, I., Kratina, T., and Kluck, R.M. (2012). Bax dimerizes via a symmetric BH3:groove interface during apoptosis. Cell Death Differ. 19, 661–670.

Du, H., Wolf, J., Schafer, B., Moldoveanu, T., Chipuk, J.E., and Kuwana, T. (2011). BH3 domains other than Bim and Bid can directly activate Bax/Bak. J. Biol. Chem. 286, 491–501.

Edlich, F., Banerjee, S., Suzuki, M., Cleland, M.M., Arnoult, D., Wang, C., Neutzner, A., Tjandra, N., and Youle, R.J. (2011). Bcl-x(L) retrotranslocates Bax from the mitochondria into the cytosol. Cell 145, 104–116.

Edwards, A.L., Gavathiotis, E., LaBelle, J.L., Braun, C.R., Opoku-Nsiah, K.A., Bird, G.H., and Walensky, L.D. (2013). Multimodal interaction with BCL-2 family proteins underlies the proapoptotic activity of PUMA BH3. Chem. Biol. 20, 888–902.

Follis, A.V., Chipuk, J.E., Fisher, J.C., Yun, M.-K., Grace, C.R., Nourse, A., Baran, K., Ou, L., Min, L., White, S.W., et al. (2013). PUMA binding induces partial unfolding within BCL-xL to disrupt p53 binding and promote apoptosis. Nat. Chem. Biol. 9, 163–168.

Gallenne, T., Gautier, F., Oliver, L., Hervouet, E., Noël, B., Hickman, J.A., Geneste, O., Cartron, P.-F., Vallette, F.M., Manon, S., and Juin, P. (2009). Bax activation by the BH3-only protein Puma promotes cell dependence on antiapoptotic Bcl-2 family members. J. Cell Biol. 185, 279–290.

Garenne, D., Renault, T., and Manon, S. (2016). Bax mitochondrial relocation is linked to its phosphorylation and its interaction with Bcl-xL. Microb. Cell 3, (in press). http://dx.doi.org/10.15698/mic2016.12.547.

Gautier, F., Guillemin, Y., Cartron, P.F., Gallenne, T., Cauquil, N., Le Diguarher, T., Casara, P., Vallette, F.M., Manon, S., Hickman, J.A., et al. (2011). Bax activation by engagement with, then release from, the BH3 binding site of Bcl-xL. Mol. Cell. Biol. 31, 832–844.

Gavathiotis, E., Suzuki, M., Davis, M.L., Pitter, K., Bird, G.H., Katz, S.G., Tu, H.-C., Kim, H., Cheng, E.H.-Y., Tjandra, N., and Walensky, L.D. (2008). BAX activation is initiated at a novel interaction site. Nature 455, 1076–1081.

Griffiths, G.J., Dubrez, L., Morgan, C.P., Jones, N.A., Whitehouse, J., Corfe, B.M., Dive, C., and Hickman, J.A. (1999). Cell damage-induced conformational changes of the pro-apoptotic protein Bak in vivo precede the onset of apoptosis. J Cell Biol. 144, 903–914.

Hockings, C., Anwari, K., Ninnis, R.L., Brouwer, J., O'Hely, M., Evangelista, M., Hinds, M.G., Czabotar, P.E., Lee, E.F., Fairlie, W.D., et al. (2015). Bid chimeras indicate that most BH3-only proteins can directly activate Bak and Bax, and show no preference for Bak versus Bax. Cell Death Dis. 6, e1735.

Hsu, Y.-T., and Youle, R.J. (1997). Nonionic detergents induce dimerization among members of the Bcl-2 family. J. Biol. Chem. 272, 13829–13834.

Ichim, G., Lopez, J., Ahmed, S.U., Muthalagu, N., Giampazolias, E., Delgado, M.E., Haller, M., Riley, J.S., Mason, S.M., Athineos, D., et al. (2015). Limited mitochondrial permeabilization causes DNA damage and genomic instability in the absence of cell death. Mol. Cell 57, 860–872.

Jeffers, J.R., Parganas, E., Lee, Y., Yang, C., Wang, J., Brennan, J., MacLean, K.H., Han, J., Chittenden, T., Ihle, J.N., et al. (2003). Puma is an essential mediator of p53-dependent and -independent apoptotic pathways. Cancer Cell 4, 321–328.

Juin, P., Geneste, O., Gautier, F., Depil, S., and Campone, M. (2013). Decoding and unlocking the BCL-2 dependency of cancer cells. Nat Rev Cancer 13, 455–465.

Kim, H., Rafiuddin-Shah, M., Tu, H.-C., Jeffers, J.R., Zambetti, G.P., Hsieh, J.J.-D., and Cheng, E.H.-Y. (2006). Hierarchical regulation of mitochondrion-dependent apoptosis by BCL-2 subfamilies. Nat. Cell Biol. 8, 1348–1358.

Le Pen, J., Laurent, M., Sarosiek, K., Vuillier, C., Gautier, F., Montessuit, S., Martinou, J.C., Letaï, A., Braun, F., and Juin, P.P. (2016). Constitutive p53 heightens mitochondrial apoptotic priming and favors cell death induction by BH3 mimetic inhibitors of BCL-xL. Cell Death Dis. 7, e2083.

Leber, B., Lin, J., and Andrews, D.W. (2010). Still embedded together binding to membranes regulates Bcl-2 protein interactions. Oncogene 29, 5221–5230.

Lessene, G., Czabotar, P.E., Sleebs, B.E., Zobel, K., Lowes, K.N., Adams, J.M., Baell, J.B., Colman, P.M., Deshayes, K., Fairbrother, W.J., et al. (2013). Structure-guided design of a selective BCL-X(L) inhibitor. Nat. Chem. Biol. 9, 390–397.

Liu, Q., Leber, B., and Andrews, D.W. (2012). Interactions of pro-apoptotic BH3 proteins with anti-apoptotic Bcl-2 family proteins measured in live MCF-7 cells using FLIM FRET. Cell Cycle 11, 3536–3542.

Llambi, F., Moldoveanu, T., Tait, S.W.G., Bouchier-Hayes, L., Temirov, J., McCormick, L.L., Dillon, C.P., and Green, D.R. (2011). A unified model of mammalian BCL-2 protein family interactions at the mitochondria. Mol. Cell 44, 517–531.

Lopez, J., Bessou, M., Riley, J.S., Giampazolias, E., Todt, F., Rochegüe, T., Oberst, A., Green, D.R., Edlich, F., Ichim, G., and Tait, S.W. (2016). Mito-priming as a method to engineer Bcl-2 addiction. Nat. Commun. 7, 10538.

Mason, K.D., Carpinelli, M.R., Fletcher, J.I., Collinge, J.E., Hilton, A.A., Ellis, S., Kelly, P.N., Ekert, P.G., Metcalf, D., Roberts, A.W., et al. (2007). Programmed anuclear cell death delimits platelet life span. Cell 128, 1173–1186.

Mérino, D., Khaw, S.L., Glaser, S.P., Anderson, D.J., Belmont, L.D., Wong, C., Yue, P., Robati, M., Phipson, B., Fairlie, W.D., et al. (2012). Bcl-2, Bcl-x(L), and Bcl-w are not equivalent targets of ABT-737 and navitoclax (ABT-263) in lymphoid and leukemic cells. Blood 119, 5807–5816.

Moldoveanu, T., Follis, A.V., Kriwacki, R.W., and Green, D.R. (2014). Many players in BCL-2 family affairs. Trends Biochem. Sci. 39, 101–111.

Nechushtan, A., Smith, C.L., Hsu, Y.-T., and Youle, R.J. (1999). Conformation of the Bax C-terminus regulates subcellular location and cell death. EMBO J. 18, 2330–2341.

Pfleger, K.D., and Eidne, K.A. (2006). Illuminating insights into protein-protein interactions using bioluminescence resonance energy transfer (BRET). Nat. Methods 3, 165–174.

Ren, D., Tu, H.-C., Kim, H., Wang, G.X., Bean, G.R., Takeuchi, O., Jeffers, J.R., Zambetti, G.P., Hsieh, J.J.-D., and Cheng, E.H.-Y. (2010). BID, BIM, and PUMA are essential for activation of the BAX- and BAK-dependent cell death program. Science 330, 1390–1393.

Rooswinkel, R.W., van de Kooij, B., Verheij, M., and Borst, J. (2012). Bcl-2 is a better ABT-737 target than Bcl-xL or Bcl-w and only Noxa overcomes resistance mediated by Mcl-1, Bfl-1, or Bcl-B. Cell Death Dis. 3, e366.

Schellenberg, B., Wang, P., Keeble, J.A., Rodriguez-Enriquez, R., Walker, S., Owens, T.W., Foster, F., Tanianis-Hughes, J., Brennan, K., Streuli, C.H., and Gilmore, A.P. (2013). Bax exists in a dynamic equilibrium between the cytosol and mitochondria to control apoptotic priming. Mol Cell 49, 959–971.

Subburaj, Y., Cosentino, K., Axmann, M., Pedrueza-Villalmanzo, E., Hermann, E., Bleicken, S., Spatz, J., and García-Sáez, A.J. (2015). Bax monomers form

OPEN
ACCESS

CellPress

dimer units in the membrane that further self-assemble into multiple oligomeric species. Nat. Commun. 6, 8042.

Todt, F., Cakir, Z., Reichenbach, F., Youle, R.J., and Edlich, F. (2013). The C-terminal helix of Bcl-x(L) mediates Bax retrotranslocation from the mitochondria. Cell Death Differ. 20, 333–342.

van Delft, M.F., Wei, A.H., Mason, K.D., Vandenberg, C.J., Chen, L., Czabotar, P.E., Willis, S.N., Scott, C.L., Day, C.L., Cory, S., et al. (2006). The BH3 mimetic ABT-737 targets selective Bcl-2 proteins and efficiently induces apoptosis via Bak/Bax if Mcl-1 is neutralized. Cancer Cell 10, 389–399.

Vogler, M., Butterworth, M., Majid, A., Walewska, R.J., Sun, X.-M., Dyer, M.J.S., and Cohen, G.M. (2009). Concurrent up-regulation of BCL-XL and BCL2A1 induces approximately 1000-fold resistance to ABT-737 in chronic lymphocytic leukemia. Blood 113, 4403–4413.

Wei, G., Margolin, A.A., Haery, L., Brown, E., Cucolo, L., Julian, B., Shehata, S., Kung, A.L., Beroukhim, R., and Golub, T.R. (2012). Chemical genomics iden-tifies small-molecule MCL1 repressors and BCL-xL as a predictor of MCL1 dependency. Cancer Cell 21, 547–562.

Wilfling, F., Weber, A., Potthoff, S., Vögtle, F.-N., Meisinger, C., Paschen, S.A., and Häcker, G. (2012). BH3-only proteins are tail-anchored in the outer mitochondrial membrane and can initiate the activation of Bax. Cell Death Differ. 19, 1328–1336.

Wilson, W.H., O'Connor, O.A., Czuczman, M.S., LaCasce, A.S., Gereci-tano, J.F., Leonard, J.P., Tulpule, A., Dunleavy, K., Xiong, H., Chiu, Y.-L., et al. (2010). Navitoclax, a targeted high-affinity inhibitor of BCL-2, in lymphoid malignancies: a phase 1 dose-escalation study of safety, phar-macokinetics, pharmacodynamics, and antitumour activity. Lancet Oncol. 11, 1149–1159.

Yao, Y., Fujimoto, L.M., Hirshman, N., Bobkov, A.A., Antignani, A., Youle, R.J., and Marassi, F.M. (2015). Conformation of BCL-XL upon Membrane Integra-tion. J. Mol. Biol. 427, 2262–2270.